View metadata, citation and similar papers at core.ac.uk

brought to you by CORE

provided by Elsevier - Publisher Connector

Available online at www.sciencedirect.com

SciVerse ScienceDirect

Energy Procedia 37 (2013) 3699 – 3710

Energy Procedia

GHGT-11

Impact of co-injected gases on CO_2 storage sites: geochemical modeling of experimental results

Jérôme Corvisier[a,*], Anne-Flore Bonvalot[a], Vincent Lagneau[a], Pierre Chiquet[b], Stéphane Renard[c,d,e], Jérôme Sterpenich[c,d], Jacques Pironon[c,d]

[a]*MINES ParisTech, Geosciences Center, 35 rue Saint-Honoré 77305 Fontainebleau cedex, France*
[b]*TOTAL, CSTJF, avenue Laribau 64018 Pau cedex, France*
[c]*Université de Lorraine, UMR7566 G2R, B.P. 70239 F-54506 Vandoeuvre-lès-Nancy, France*
[d]*CNRS, UMR7566 G2R, B.P. 70239 F-54506 Vandoeuvre-lès-Nancy, France*
[e]*IFP Energies Nouvelles, 1 & 4 avenue de Bois-Préau 92852 Rueil-Malmaison cedex, France*

Abstract

At the end of a CO_2 capture process the gas mixture composition can vary considerably incorporating components such as O_2, N_2, SO_x, H_2S, N_yO_x, H_2, CO, Ar at various concentration levels. These impurities, even if their concentrations are not significant from a health perspective, could lead to significant chemical reactivity towards reservoir or caprock minerals and well materials. Potential processes and impacts are not well documented yet. However, in the near future, it will be crucial for both operators and regulators to rely on numerical reactive-transport simulations able to model the behavior of these complex systems and consequently able to ensure the long-term stability of storage sites. Furthermore, numerous modeling studies have shown how limiting it could be to consider simple assumptions for gases such as ‘‘dissolved gases only’’ or ‘‘infinite sources of gas’’, and also how important it is to correctly handle the gaseous phase.

Recently, within the GAZ ANNEXES project funded by the ANR (French national research agency), we developed gas modules for both the geochemical code CHESS and the coupled reactive/transport code HYTEC. These advances make it now possible to simulate water/gas/rock interactions accurately.

Within this project, some of the potential co-injected impurities were experimentally studied, highlighting their influence on the geochemical reactivity of some carbonate rocks involved in CCS. In this paper, the new gas module of CHESS is presented as well as its ability to reproduce these experimental results giving an important help to study both qualitatively and quantitatively the impact of co-injected gases. One key result for the experiments involving a gas mixture (82%mol $CO_{2(g)}$, 6% $Ar_{(g)}$, 4% $N_{2(g)}$, 4% $SO_{2(g)}$ and 4% $O_{2(g)}$), which are the closest to real operations: both experimental and numerical results indicate a relative low reactivity of the rock.

© 2013 The Authors. Published by Elsevier Ltd.
Selection and/or peer-review under responsibility of GHGT

Keywords: Water/gas/rock interactions, geochemical modeling, co-injected gases

* Corresponding author. Tel.: +33-164-694-750; fax: +33-164-694-713.
E-mail address: Jerome.corvisier@mines-paristech.fr.

1876-6102 © 2013 The Authors. Published by Elsevier Ltd.
Selection and/or peer-review under responsibility of GHGT
doi:10.1016/j.egypro.2013.06.264

1. Introduction

At the end of a CO_2 capture process the gas mixture composition can vary considerably both qualitatively and quantitatively, based on the specific industrial emitter and the capture technology. In addition to CO_2, several components such as O_2, N_2, SO_x, H_2S, N_yO_x, H_2, CO, Ar can be present at various concentration levels [1]. These impurities, even if their concentrations are not significant from a health perspective, could lead to significant chemical reactivity towards reservoir or caprock minerals and well materials [2-10]. Potential processes and impacts are not well documented yet. However, in the near future, it will be crucial for both operators and regulators to rely on numerical reactive-transport simulations able to model the behavior of these complex systems and consequently able to ensure the long-term stability of storage sites. Furthermore, numerous modeling studies have shown how limiting it could be to consider simple assumptions for gases such as "dissolved gases only" or "infinite sources of gas", and also how important it is to correctly handle the gaseous phase.

Within the GAZ ANNEXES project funded by the ANR (French national research agency), we developed gas modules for both the geochemical code CHESS [11] and the coupled reactive/transport code HYTEC [12]. These advances make it now possible to simulate water/gas/rock interactions accurately [13]. Recently, within this same project, Renard and co-workers [5-7] experimentally studied some of the potential co-injected impurities and their influence on the geochemical reactivity of some carbonate rocks involved in CCS.

In this paper, we first focus on the brief presentation of the recent numerical development of CHESS and its new gas module that enables us to simulate real gases and their interactions with water and rocks in either constant volume or pressure conditions. In a second step, the ability of this code to reproduce the experiments of Renard [5-7] is tested and, experimental and numerical results are compared.

2. Modeling water/gas/rock interactions using CHESS/HYTEC

In most geochemical codes, gases are considered as infinite reservoirs and it is therefore equivalent to fix the corresponding dissolved concentrations in the aqueous solution. This assumption appears to be realistic when modeling open or semi-open reactors in which gases are continuously pumped in to maintain the global pressure constant, or for a shallow aquifer in contact with the atmosphere. In fact, the mass balances involving gaseous species are not taken into account and the dissolved aqueous species just obey the corresponding mass action law. The system of equations that has to be solved is much simpler. Nevertheless, for closed reactors or for every general two-phase reactive-transport problems, this approach cannot be satisfactory.
Consequently, CHESS, the geochemical core of HYTEC, has been improved [13] and proposes now three different options to simulate water/gas/rock interactions:

- Infinite source of gas;
- Finite source of gas at a constant volume;
- Finite source of gas at a constant pressure.

In all these configurations, the gas-liquid equilibrium is assumed. For example, the reaction of dissolution of carbon dioxide into the aqueous solution:

$$CO_{2(aq)} \leftrightarrow CO_{2(g)} \tag{1}$$

imposes its associated mass action law in a dissymetric (fugacity-activity) approach:

$$f_{CO_{2(g)}} = \phi_{CO_{2(g)}} Y_{CO_{2(g)}} P = K_{CO_{2(g)}} \left\{CO_{2(aq)}\right\} \tag{2}$$

where f is the fugacity, ϕ the fugacity coefficient, Y the mole fraction in the gas phase, P the total pressure, K the equilibrium constant for reaction (1) and $\{.\}$ the activity of a dissolved (liquid phase) species.

If a finite source of gas is considered, gas components must step in the mass balances. To do so, it is necessary to implement a relationship between pressure, temperature and the quantity of each components of a gas mixture, using an equation of state (EOS). The perfect gas approximation can be sufficiently accurate for some applications (*i.e.* low pressure/low temperature), but cubic equations, such as the Peng-Robinson EOS for example [14] are more precise and often required:

$$P = \frac{RT}{V(V+b)} + \frac{a(T)}{V(V+b)+b(V-b)} \tag{3}$$

where V is the molar volume of the compressed gas phase at P and T, and R the gas constant. a and b represent intermolecular attraction and repulsion and are calculated from all the a_i and b_i of each components of the gas phase derived from critical parameters using a mixing rule:

$$a = \sum_i \sum_j Y_i Y_j (a_i)^{1/2} (a_j)^{1/2} (1-k_{ij}) \tag{4a}$$

$$b = \sum_i Y_i b_i \tag{4b}$$

k_{ij} are the binary interactions parameters for the component i and j in the gas phase.

When the volume is fixed, the molar volume gives straightforward access to pressure. Alternatively, when the pressure is fixed, it is a bit more complex to calculate the molar volume. However, rewriting (3) as a general cubic equation in terms of volume, it can be solved directly using the Cardan's method [15,16] while more complex equations of state imply iterative resolution and are then less adapted for reactive-transport codes.

As an example, the fugacity coefficient for $CO_{2(g)}$ in a mixture, when considering the Peng-Robinson EOS (3) and these mixing rule, can be written as follows:

$$\ln \phi_{CO_{2(g)}} = \frac{b_{CO_{2(g)}}}{b}\left(\frac{PV}{RT}-1\right) - \ln\left(\frac{PV}{RT}-\frac{Pb}{RT}\right) - \frac{a}{2\sqrt{2}RTb}\left(\frac{2\sqrt{a_{CO_{2(g)}}}\sum_i Y_i\sqrt{a_i}\left(1-k_{iCO_{2(g)}}\right)}{a} - \frac{b_{CO_{2(g)}}}{b}\right) \times \ln\left(\frac{V+\left(1+\sqrt{2}\right)b}{V+\left(1-\sqrt{2}\right)b}\right) \tag{5}$$

The new version of CHESS including this gas module already showed its ability to reproduce various water/gas solubility experiments and also rather simple water/gas/rock reactivity experiments [13]. It shall now be tested on much more complex systems involving minerals assemblages and gas mixtures.

3. Application to water/gas/rock reactivity experiments

3.1. Description of the experiments

Still within the GAZ ANNEXES project funded by the ANR, some experimental researches were performed in order to evaluate the influence of impurities potentially co-injected along with the $CO_{2(g)}$ for its geological storage on the geochemical reactivity of rocks [5-7]. These experiments were performed in batch reactors (2 cm^3 gold capsules) containing a mineral assemblage within a 25 $g.L^{-1}$ NaCl brine and in contact with a gas phase at 150°C and 100 bar during 1 month. Various sets of gases including a gas

mixture and different mineral assemblages including a realistic natural dolomitic rock sample were tested. Among other experiments, some runs were selected as validation cases for the new code.
The reactivity of a first synthetic assemblage, S1, composed of 99%mol dolomite and 1% pyrite was tested versus pure $N_{2(g)}$, pure $CO_{2(g)}$, pure $SO_{2(g)}$ and a gas mixture composed of 82%mol $CO_{2(g)}$, 6% $Ar_{(g)}$, 4% $N_{2(g)}$, 4% $SO_{2(g)}$ and 4% $O_{2(g)}$. The initial quantities of gas water, NaCl and minerals for these experiments are summed up in Table 1.

Table 1. Initial quantities of gas, water, salt and minerals in the capsules for the experiments run on the synthetic assemblage S1

Gas compound	Gas (mol)	H_2O (mol)	NaCl (mol)	dolomite (mol)	pyrite (mol)	quartz (mol)
$N_{2(g)}$	$7.14\ 10^{-4}$	$3.43\ 10^{-2}$	$2.65\ 10^{-4}$	$7.00\ 10^{-4}$	$7.07\ 10^{-6}$	$8.32\ 10^{-4}$
$CO_{2(g)}$	$5.57\ 10^{-3}$	$3.47\ 10^{-2}$	$2.67\ 10^{-4}$	$7.00\ 10^{-4}$	$7.07\ 10^{-6}$	$8.32\ 10^{-4}$
$SO_{2(g)}$	$7.84\ 10^{-3}$	$3.39\ 10^{-2}$	$2.62\ 10^{-4}$	$7.00\ 10^{-4}$	$7.07\ 10^{-6}$	$9.99\ 10^{-4}$
Mixture	$2.30\ 10^{-3}$	$2.71\ 10^{-2}$	$2.09\ 10^{-4}$	$5.39\ 10^{-4}$	$5.44\ 10^{-6}$	$2.33\ 10^{-4}$

Another synthetic assemblage, S2, composed of 96.00%mol calcite, 3.84% muscovite and 0.16% paragonite, was tested with the same gases and the initial quantities of the corresponding experiments appear in Table 2. An initial mixture between muscovite $(Si_3Al)(Al_2)KO_{10}(OH)_2$ and paragonite $(Si_3Al)(Al_2)NaO_{10}(OH)_2$ is considered in order to be able to reproduce the slight sodium enrichment observed during the experiment.

Table 2. Initial quantities of gas, water, salt and minerals in the capsules for the experiments run on the synthetic assemblage S2

Gas compound	Gas (mol)	H_2O (mol)	NaCl (mol)	calcite (mol)	muscovite (mol)	paragonite (mol)	quartz (mol)
$N_{2(g)}$	$2.49\ 10^{-4}$	$3.41\ 10^{-2}$	$2.63\ 10^{-4}$	$8.57\ 10^{-4}$	$3.43\ 10^{-5}$	$1.43\ 10^{-6}$	$4.99\ 10^{-4}$
$CO_{2(g)}$	$3.52\ 10^{-3}$	$2.73\ 10^{-2}$	$2.11\ 10^{-4}$	$8.57\ 10^{-4}$	$3.43\ 10^{-5}$	$1.43\ 10^{-6}$	$2.50\ 10^{-4}$
$SO_{2(g)}$	$9.05\ 10^{-3}$	$2.87\ 10^{-2}$	$2.21\ 10^{-4}$	$8.66\ 10^{-4}$	$3.46\ 10^{-5}$	$1.44\ 10^{-6}$	$4.99\ 10^{-4}$
Mixture	$2.30\ 10^{-3}$	$2.71\ 10^{-2}$	$2.09\ 10^{-4}$	$8.66\ 10^{-4}$	$3.46\ 10^{-5}$	$1.44\ 10^{-6}$	$2.33\ 10^{-4}$

Finally, experiments involving a natural dolomitic rock and the same set of gases were also retained. Recent work was done on its characterization for the purpose of improving geochemical models [10]. The resulting composition of these efforts is 89.77%mol dolomite $CaMg(CO_3)_2$, 0.95% calcite $CaCO_3$, 7.42% quartz SiO_2, 0.53% pyrite FeS_2, 0.08% fluorapatite $Ca_5F(PO_4)_3$, 0.21% sudoite $(Al_3Mg_2)(Si_3Al)O_{10}(OH)_8$, 0,34% muscovite $(Si_3Al)(Al_2)KO_{10}(OH)_2$, 0.63% montmorillonite-Na $(Al_{1.67}Na_{0.33}Mg_{0.33})Si_4O_{10}(OH)_2$ and 0.07% hematite Fe_2O_3. The initial quantities for the experiments are presented in Table 3.

Table 3. Initial quantities (mol.) of gas, water, salt and main minerals in the capsules for the experiments run on the natural assemblage RES

Gas comp.	Gas	H_2O	NaCl	Dol.	Cal.	Qua.	Pyr.	Sud.	Mus.	Mon.
$N_{2(g)}$	$7.14\ 10^{-4}$	$3.43\ 10^{-2}$	$2.65\ 10^{-4}$	$6.75\ 10^{-4}$	$7.14\ 10^{-6}$	$9.38\ 10^{-4}$	$3.99\ 10^{-6}$	$1.54\ 10^{-6}$	$2.57\ 10^{-6}$	$4.77\ 10^{-6}$
$CO_{2(g)}$	$5.57\ 10^{-3}$	$3.47\ 10^{-2}$	$2.67\ 10^{-4}$	$6.60\ 10^{-4}$	$6.99\ 10^{-6}$	$1.05\ 10^{-3}$	$3.90\ 10^{-6}$	$1.51\ 10^{-6}$	$2.52\ 10^{-6}$	$4.67\ 10^{-6}$
$SO_{2(g)}$	$7.84\ 10^{-3}$	$3.39\ 10^{-2}$	$2.62\ 10^{-4}$	$5.08\ 10^{-4}$	$5.73\ 10^{-6}$	$7.24\ 10^{-4}$	$3.00\ 10^{-6}$	$1.16\ 10^{-6}$	$1.94\ 10^{-6}$	$3.59\ 10^{-6}$

Mix.	$2.30\ 10^{-3}$	$2.71\ 10^{-2}$	$2.09\ 10^{-4}$	$6.75\ 10^{-4}$	$7.15\ 10^{-6}$	$1.19\ 10^{-3}$	$3.99\ 10^{-6}$	$1.54\ 10^{-6}$	$2.57\ 10^{-6}$	$4.77\ 10^{-6}$

It is important to note here that the quantification of mineral phases and the global mass balances at the end of the experiments are done using the measured aqueous concentrations and a defined mineralogy, determined with the help of SEM images and analyses and some XRD measurements.
In the following section, both experimental and numerical results are exposed and compared with each other.

3.2. Numerical simulations and comparison with experimental results

In order to try to reproduce the experimental results, we use CHESS and its newly developed gas module briefly introduced earlier in this paper, along with the SLOP98 database (http://geopig.asu.edu/sites/default/files/slop98.dat), except for the natural assemblage where the thermodynamic constants comes from [17]. For activity corrections, various models were selected: the B-dot model [18] for aqueous species, the model of Helgeson [18] for water and the Peng-Robinson model [14] for gases.

- Synthetic assemblage S1

The obtained results for both the experiments performed by Renard [5] and the numerical simulations run with CHESS on the synthetic assemblage S1 are presented together on the Fig 1. We observe a very good agreement between experimental and numerical results whatever the set of gases considered. Simulations allow then to analyze the various mechanisms involved during the different experiments.

υ $N_{2(g)}$

The dissolution of nitrogen in the aqueous solution produces some minor quantity of $O_{2(aq)}$ which, combined with the small residual amount of oxygen despite the initial vacuum (between 10 and 30 mbar), oxidizes some pyrite into hematite (see Fig 1A):

$$2\text{pyrite}+4H_2O+\frac{15}{2}O_{2(aq)} \leftrightarrow \text{hematite}+4SO_4^{2-}+8H^+ \quad (6)$$

Numerically, this imprecise initial quantity of $O_{2(aq)}$ can be adjusted to reproduce the experimentally observed quantity of hematite.
The resulting slight acidification of the aqueous solution generates then the dissolution of a little amount of dolomite (see Fig 1A). In these conditions (*i.e.* pH and pe), SO_4^{2-} and Na^+ ions combine to form $NaSO_4^-$ (see Fig 1C):

$$SO_4^{2-}+Na^+ \leftrightarrow NaSO_4^- \quad (7)$$

There is a noticeable presence of $H_2O_{(g)}$ in the simulated gas phase (as in all other simulations), unfortunately water was not analyzed in the collected gas samples.

υ $CO_{2(g)}$

The carbon dioxide dissolves in the aqueous solution, lowering its pH and occasioning the dissolution of some dolomite. As mentioned previously, the presence of some residual oxygen in the experiments leads to the formation of hematite from pyrite (6) and of $NaSO_4^-$ (7).
Since no siderite has been observed in this experiment, siderite is not allowed to precipitate in the simulation although it tends to form in these conditions.

υ $SO_{2(g)}$

The dissolution of sulfur dioxide lowers significantly the pH of the aqueous solution and dolomite consequently dissolves. Moreover, once dissolved, the sulfur disproportionates and then leads to the formation of solid sulfur (see Fig 1A):

$$3SO_{2(g)}+2H_2O \leftrightarrow 2HSO_4^-+S(\text{alpha})+2H^+ \quad (8)$$

Finally, Ca^{2+} cations from the dolomite dissolution react with HSO_4^- to form anhydrite and also pursue the acidification of the aqueous solution:

$$Ca^{2+} + HSO_4^- \leftrightarrow \text{anhydrite} + H^+ \quad (9)$$

In this experiment, reactions are total and this allows the accurate reproduction of mineral quantities.

The presence of $SO_{2(g)}$ in the gas phase after the experiment shall be noticed although there is no $SO_{2(g)}$ in the simulated gas phase. This can be explained by the method used to collect the gas phase before its analysis using Raman spectrometry, which implies a degassing with an important decrease of pressure and then induces a perturbation of the water/gas/rock equilibrium. However, the analyses of some synthetic fluid inclusions show that $SO_{2(g)}$ is completely dissolved in the aqueous phase in these experimental conditions [5], consistently with the numerical behavior. It shall also be noticed that the ionic strength for this system is very high (around 10 molal) and activity correction models for aqueous species such as B-dot [18] are then out of their validity range.

υ Gas mixture

In this experiment $SO_{2(g)}$ and $O_{2(g)}$ dissolve into water and lower significantly the pH of the aqueous phase, leading to the dissolution of dolomite and the transformation of pyrite into hematite. Since the amount of oxygen is important, pyrite completely disappears. Then, SO_4^{2-}, produced by the oxidation of $SO_{2(aq)}$, combines with Ca^{2+} and Mg^{2+}, from the dolomite dissolution, to form anhydrite and $MgSO_{4(aq)}$:

$$Ca^{2+} + Mg^{2+} + 2SO_4^{2-} \leftrightarrow \text{anhydrite} + MgSO_{4(aq)} \quad (10)$$

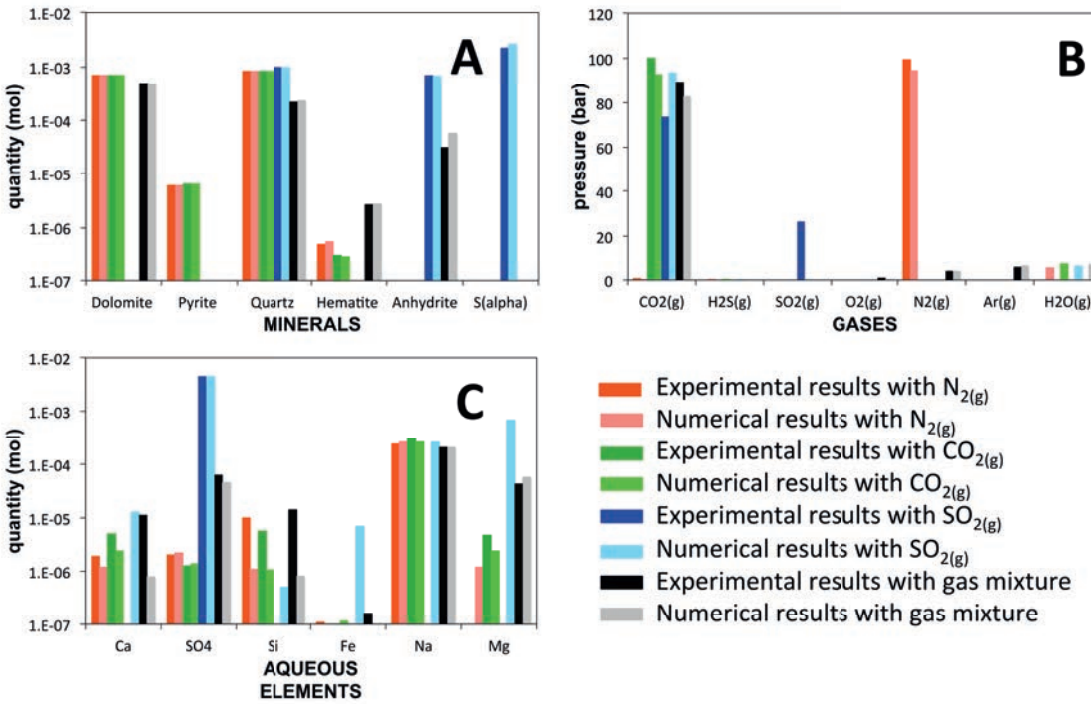

Fig. 1. Comparison between experimental and numerical results obtained for synthetic assemblage S1 (A) minerals; (B) gases and (C) aqueous solution

In this last experiment for the synthetic assemblage S1, there is no $O_{2(g)}$ in the simulated gas phase, while oxygen is detected after the experiment using Raman spectrometry. Here again, the inevitable degassing to collect the gas phase can explain this difference.

If we focus on the role of the impurities comparing the experiment with pure $CO_{2(g)}$ and the experiment with the gas mixture, we observe that with the co-injected gases more dolomite is dissolved (approximately -10%mol for the mixture compared to -1% for pure $CO_{2(g)}$), pyrite is totally dissolved (-100%mol compared to -10%), more hematite precipitates and also anhydrite forms. All is majorly linked to the presence of oxidizing gases such as $SO_{2(g)}$ and $O_{2(g)}$ which have a direct and important impact on minerals like pyrite, and also to the acidifying role of $SO_{2(g)}$ which enhances a little the dissolution of dolomite and produces anhydrite.

- Synthetic assemblage S2

Experimental and numerical results for this synthetic assemblage S2 are presented on Fig 2 and are in good agreement too. The various involved mechanisms can also be investigated for each gas.

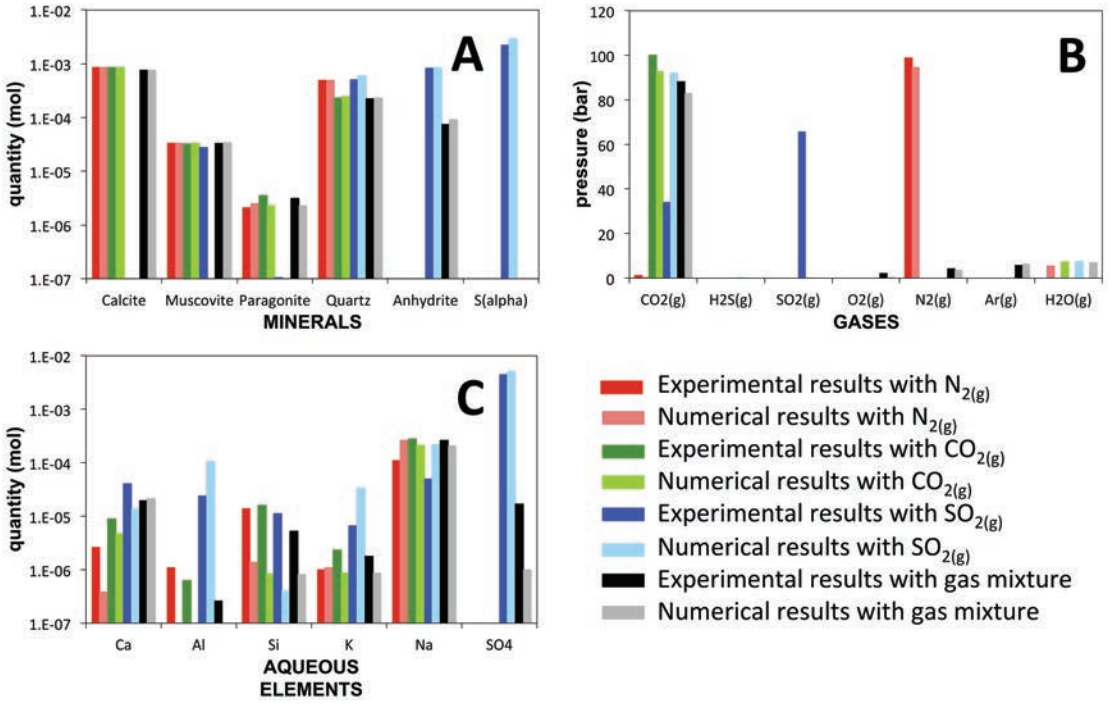

Fig. 2. Comparison between experimental and numerical results obtained for synthetic assemblage S2 (A) minerals; (B) gases and (C) aqueous solution

- $N_{2(g)}$

As for the synthetic assemblage S1, the nitrogen dissolution produces a little amount of $O_{2(aq)}$, but there is no oxidizable mineral in this assemblage. A very slight amount of calcite is dissolved to reach equilibrium. Muscovite dissolves as well, while paragonite tends to precipitate noticeably (see Fig 2A). The numerical simulation particularly succeeds in reproducing qualitatively and quantitatively this combined sodium enrichment and potassium depletion.

υ $CO_{2(g)}$

The carbon dioxide dissolves in the aqueous solution, lowering its pH and more calcite is consequently dissolved. Here also, a sodium enrichment and potassium depletion of the muscovite/paragonite assemblage is observed both experimentally and numerically.

υ $SO_{2(g)}$

The same behavior as the one seen with the synthetic assemblage S1 is observed. The sulfur dioxide dissolves, lowers significantly the pH of the aqueous solution, the sulfur disproportionates once dissolved and then leads to the formation of solid sulfur. Due to important water acidification, the calcite dissolves completely and then releases Ca^{2+} ions that combine with HSO_4^- to form anhydrite.

It seems that muscovite is preserved at the end of the experiment, while it is completely dissolved in the simulation (see Fig 2A). This is probably due to fact that the muscovite dissolution is kinetically controlled, while only thermodynamic equilibrium is considered in our calculus.

As previously explained, the observation of $SO_{2(g)}$ at the end of the experiment (see Fig 2B) is probably due to the degassing that occurs during the gas phase collection.

υ Gas mixture

$SO_{2(g)}$ and $O_{2(g)}$ dissolve and lower significantly the pH of the aqueous, leading to the dissolution of calcite. The SO_4^{2-}, produced by the oxidation of $SO_{2(aq)}$, combines with Ca^{2+}, from the calcite dissolution, to form anhydrite and $CaSO_{4(aq)}$ (see Fig 2A):

$$2Ca^{2+} + 2SO_4^{2-} \leftrightarrow \text{anhydrite} + CaSO_{4(aq)} \quad (11)$$

As mentioned in the simulation with the synthetic assemblage S1, the method used to collect the gas phase can explain the presence of $O_{2(g)}$ at the end of the experiment, non numerically reproducible.

Comparing the pure $CO_{2(g)}$ and the gas mixture experiments, we only notice that, when some impurities are present, more calcite is dissolved (more than -10%mol for -1% for pure $CO_{2(g)}$) and some anhydrite appears. Since there is no oxidizable minerals in this assemblage, the presence of $SO_{2(g)}$ enhances a little the acidification of the aqueous solution and consequently the calcite dissolution as well as the anhydrite formation.

- Natural assemblage RES

Fig 3 present the results for both the experiments carried out by Renard [5-7] and the CHESS numerical simulations with the natural assemblage RES. We shall regret here a lack of information on the quantitative mineralogy of the clay minerals in these samples before and after the experiment, given the fact that characterizing these minerals is quite challenging. Even though precise data have been collected using TEM analyses giving hints on the global composition of the clay fraction. The experimental mineral quantities are then calculated from the aqueous measurements, based on a mineralogy established from these few observations. As a consequence, the experimental results for minerals directly depend on this choice. Nonetheless, even for these relatively complex systems, numerical simulations globally correlate experimental results.

υ $N_{2(g)}$

With the retained assemblage, the measured aqueous concentrations (see Fig 3C) seem to indicate the following behavior for minerals in the experiment (see Fig 3A). Concerning carbonates, dolomite slightly dissolves while calcite precipitates. For clay minerals, muscovite partly dissolves, montmorillonite-Na completely disappears and sudoite significantly precipitates. It shall also be noticed that pyrite and fluorapatite dissolve, and hematite precipitates a little. All these observations are reproduced numerically, although the precipitation

of calcite, the dissolution of muscovite and the formation of hematite are overestimated, while fluorapatite remains unaffected. Nevertheless, the simulated global depletion in sodium and potassium of clay minerals as well as their enrichment in aluminum are in good agreement with TEM analyses.

The gas phase shows a slight $CO_{2(g)}$ degassing (see Fig 3B) quite well reproduced even though it seems underestimated a bit, probably linked to the overestimation of the precipitated calcite.

As mentioned sooner, some reactions may be kinetically controlled and it may explain these noticed differences between experimental results and numerical predictions.

υ $CO_{2(g)}$

The quantification of minerals after the experiment demonstrates that a few amount of dolomite precipitates, calcite dissolves completely, muscovite and fluorapatite partly dissolves, montmorillonite-Na, sudoite and pyrite completely disappear, hematite significantly precipitates while anhydrite and kaolinite appear (see Fig 3C). The formation of kaolinite can be explained from the dissolution of sudoite in such conditions:

$$\text{sudoite} + 4H^+ + SiO_{2(aq)} \leftrightarrow \text{kaolinite} + 2Mg^{2+} + 2H_2O \quad (12)$$

All these observations are qualitatively and quantitatively simulated, however muscovite completely disappears and fluorapatite is still unaffected in our simulation. For clay minerals, the depletion in magnesium, potassium and sodium is rather well simulated.

It shall be noticed here, that Renard identified pyrite and calcite crystals on SEM images after experiments [5], which could tend to indicate that kinetics for some reactions may be considered but moreover that much further investigations shall be conducted in order to better characterize such complex assemblages.

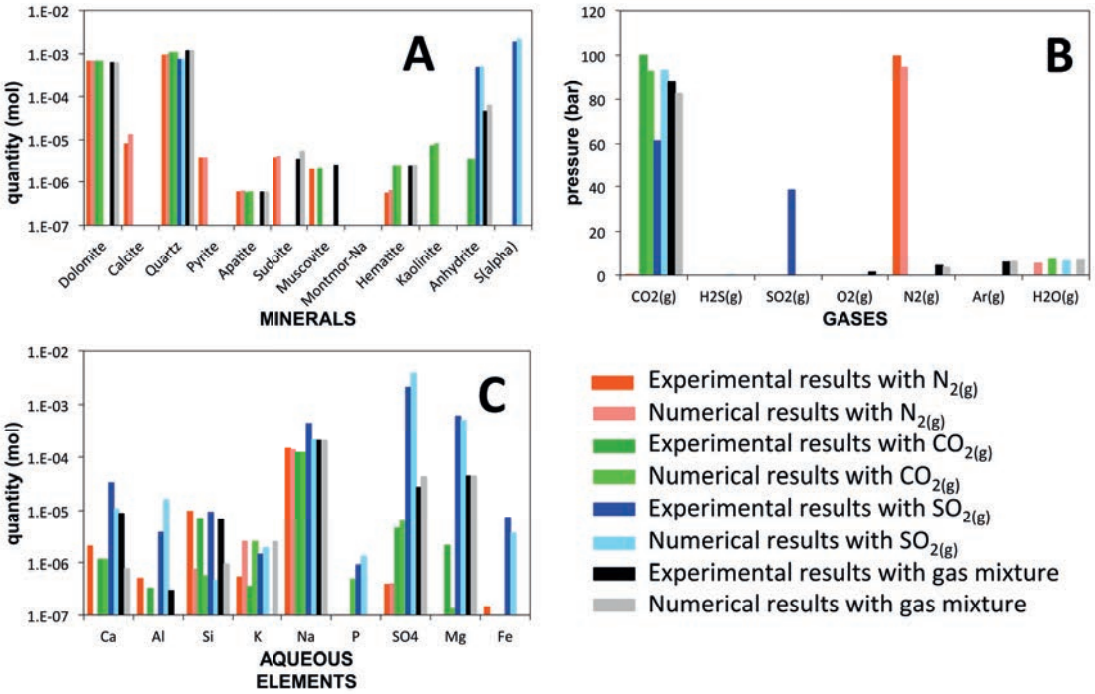

Fig. 3. Comparison between experimental and numerical results obtained for natural assemblage RES (A) minerals; (B) gases and (C) aqueous solution

- $SO_{2(g)}$

In this experiment, it seems that every mineral except quartz is dissolved (see Fig 3C). As in the previous examples with pure $SO_{2(g)}$, the dissolved sulfur disproportionates and consequently forms solid sulfur and anhydrite.
For the same technical reasons, some $SO_{2(g)}$ is detected at the end of experiment while it does not appear in the simulation. Nevertheless, some synthetic fluid inclusions analyses tend to demonstrate that $SO_{2(g)}$ was quickly dissolved during the experiments [7], in good agreement with the simulations.

- Gas mixture

During this last experiment, which is the closest to real operations, dolomite dissolves a little while calcite dissolves completely, muscovite seems unaffected, fluorapatite slightly dissolves, montmorillonite-Na and pyrite completely disappear, hematite and sudoite significantly precipitate while anhydrite appears. These experimental observations are still qualitatively and quantitatively reproduced numerically, while the precipitation of sudoite is overestimated and muscovite is totally dissolved, possibly linked to kinetic control processes.
For clay minerals, the depletion in sodium as well as the enrichment in aluminum observed on TEM analyses are also reproduced here, while the depletion in potassium is numerically overestimated due to the total dissolution of muscovite.
Once again, the technique used to collect the gas phase probably explains the difference between the quantity of $SO_{2(g)}$ obtained experimentally and numerically.

If we try to analyze the influence of the impurities comparing the pure $CO_{2(g)}$ experiment with the gas mixture experiment, we mainly notice that dolomite dissolves instead of a slight precipitation in the case of pure CO_2 (around -7.5%mol for the mixture and 0.7% for pure $CO_{2(g)}$). Regarding clay minerals, there are also some differences, since sudoite abundantly precipitates for the mixture while it dissolves totally and is transformed in kaolinite for pure $CO_{2(g)}$. The behavior of muscovite between the two experiments varies a bit, since it seems unaffected for the mixture and it dissolves for pure $CO_{2(g)}$. Nevertheless muscovite dissolves completely for both simulations. In the case of the mixture, more anhydrite forms. Here, there are various minerals concerned by redox reactions, but the impact of adding $SO_{2(g)}$ and $O_{2(g)}$ seems to be important on clay minerals such as sudoite and kaolinite. $SO_{2(g)}$ also has an influence on the behavior of carbonates since its role on the acidification of the aqueous solution forces the dolomite to dissolve.

4. Conclusions

As a conclusion, we shall first emphasize that the results turn out to be very satisfactory. Indeed, experiments and simulations match rather well. For synthetic mineral assemblages, numerical simulations experimental results are in very good agreement, qualitatively and quantitatively, in terms of mineralogical, aqueous and gaseous compositions. Then, for real reservoir samples, the mineralogy is much more complex and the lack of input key data (*i.e.* incomplete phase by phase quantification and unreliable equilibrium constants for clay minerals) made the complete validation of our modeling assumptions difficult. Nevertheless, most of the observations were matched: simulations predict carbonate dissolution, pyrite oxidation/hematite precipitation, anhydrite or even native sulfur deposit in the case of pure SO_2 gas phase. Some discrepancies may even be explained by the necessary depressurization/cooling of the gas sample before its analysis or by probable kinetic control for some mineral reactions.

The approach may also be highlighted because being able to compare our numerical results with experiments on such cases with increasing complexity is a tremendous help to handle the involved geochemical mechanisms correctly. Now, our model has been tested on different systems and the obtained results have been compared to various experimental results from gas solubility measurements [13] to rather complex reactivity experiments including brine, real rock sample and a gas mixture.

If we focus on the possibly co-injected impurities, this study allows us to underline the small impact of $SO_{2(g)}$ on the dissolution of carbonates and of $SO_{2(g)}$ and $O_{2(g)}$ on redox reactions in general and on clay minerals in our example. However, the behaviors with (unrealistic) pure $SO_{2(g)}$ and with the gas mixture (4%mol $SO_{2(g)}$) are completely different. The experiment involving the natural dolomitic rock and the gas mixture is the closest to real operations of injection and it shall be noticed that both experimental and numerical results indicate a relative low reactivity of the rock.

In the near future, we will keep collecting experimental results with accurately acquired mineralogy and trying to model them in order to validate our approach. The next step would then be to include kinetics when necessary and also to consider transport and flow in our simulations.

Acknowledgements

This work is supported by TOTAL and has been initiated during the project 'Gaz Annexes' ANR-06-CO2-005 (French national research agency).

References

[1] IEAGHG. Effects of impurities on geological storage of CO_2, *Technical Report, IEAGHG*, june 2011; **2011/04**.

[2] Heeschen K, Risse A, Ostertag-Henning C, Stadler S. Importance of co-captured gases in the underground storage of CO2: quantification of mineral alterations in chemical experiments, *Energy Procedia* 2011; **4**, p. 4480-4486.

[3] Jacquemet H, Pironon J, Caroli E. A new experimental procedure for simulation of H2S+CO2 geological storage. Application to well cement aging, *Oil & Gas Science and Technology – Rev.IFP* 2005; **60**, p. 193-206.

[4] Knauss KG, Johnson JW, Steefel CI. Evaluation of the impact of CO_2, co-contaminant gas, aqueous fluid and reservoir rock interactions on the geologic sequestration of CO_2, *Chemical Geology* 2005; **217**, p. 339-350.

[5] Renard S. Rôle des gaz annexes sur l'évolution géochimique d'un site de stockage de CO_2. Application à des réservoirs carbonatés. INPL, Nancy - France. *PhD Thesis* 2010; 422 p.

[6] Renard S, Sterpenich J, Pironon J, Chiquet P, Lescanne M, Randi A. Geochemical study of the reactivity of a carbonate rock in a geological storage of CO_2: Implications of co-injected gases, *Energy Procedia* 2011; **4**, p. 5364-5369.

[7] Renard S, Sterpenich J, Pironon J, Randi A, Chiquet P, Lescanne M. Impact of SO_2 and NO on carbonated rocks submitted to a geological storage of CO_2: an experimental study, in : Wu Y, Carroll JJ & Du Z. (Ed.) *Acid Gas Injection and Related Technologies, Calgary (AB Canada)* 2011; p. 377-392.

[8] Xu T, Apps JA, Pruess K, Yamamoto H. Numerical modeling of injection and mineral trapping of CO_2 with H_2S and SO_2 in a sandstone formation, *Chemical Geology* 2007; **242**, p. 319-346.

[9] Xiao Y, Xu T, Pruess K. The effects of gas-fluid-rock interactions on CO2 injection and storage: insights from reactive transport modeling, *Energy Procedia* 2009; **1**, p. 1783-1790.

[10] Wilke FDH, Vasquez M, Wiersberg T, Naumann R, Erzinger J. On the interaction of pure and impure supercritical CO2 with rock forming minerals in saline aquifers: An experimental geochemical approach, *Applied Geochemistry* 2012; **27**, p. 1615-1622.

[11] van der Lee J. Thermodynamic and mathematical concepts of CHESS, *Technical report, MINES ParisTech* 2009; **RT-20093103-JVDL**.

[12] van der Lee J, De Windt L, Lagneau V, Goblet P. Module-oriented modeling of reactive transport with HYTEC, *Computers & Geosciences* 2003; **29**, p. 265-275.

[13] Corvisier J, Bonnaud E, Lagneau V. Tackling water/gas/rock interactions for reactive-transport codes – An insight into the CHESS/HYTEC codes, *Proceedings Geofluids VII Reuil-Malmaison (France)* 2012; p. 67-70.

[14] Peng D-Y, Robinson DB. A new two-constant equation of state, *Industrial & Engineering Chemistry Fundamentals* 1976; **15**, p. 59-64.

[15] Nickalls RWD. A new approach to solving the cubic: Cardan's method revealed, *the Mathematical Gazette* 1993; **77**, p. 354-359.

[16] Spycher N, Pruess K, Ennis-King J. CO_2-H_2O mixtures in the geological sequestration of CO_2. I. Assessment and calculation of mutual solubilitites from 12 to 100°C and up to 600 bar, *Geochimica et Cosmochimica Acta* 2003; **67**, p. 3015-3031.

[17] Chiquet P, Thibeau S, Lescanne M, Prinet C. Geochemical assessment of the injection of CO_2 into Rousse depleted gas reservoir. Part II: Geochemical impacts of the CO_2 injection, *GHGT-11 Kyoto (Japan), 18-22 november 2012.*

[18] Helgeson H. Thermodynamics of hydrothermal systems at elevated temperatures and pressures, *American Journal of Science* 1969; **267**, p. 724-804.